

Experimental study of high energy electron interactions in a superconducting aluminum alloy resonant bar

M. Barucci^{f,g} M. Bassan^{b,c} B. Buonomo^a G. Cavallari^d
 E. Coccia^{b,c} S. D'Antonio^b V. Fafone^{b,c} C. Ligi^a L. Lolli^{f,g}
 A. Marini^a G. Mazzitelli^a G. Modestino^a G. Pizzella^{c,a}
 L. Quintieri^a L. Risegari^{f,g,1} A. Rocchi^b F. Ronga^a P. Valente^e
 G. Ventura^{f,g} S.M. Vinko^{a,2}

^a*INFN (Istituto Nazionale di Fisica Nucleare) Laboratori Nazionali di Frascati, I 00044 Frascati, Italy*

^b*INFN Sezione Roma2, I 00133 Rome, Italy*

^c*Dipartimento di Fisica, Università di Tor Vergata, I 00133 Rome, Italy*

^d*CERN, CH1211 Geneva, Switzerland*

^e*INFN Sezione di Roma1, I 00185 Rome, Italy*

^f*INFN Sezione di Firenze, I 00185 Sesto Fiorentino, Florence, Italy*

^g*Dipartimento di Fisica, Università di Firenze, I 00185 Sesto Fiorentino, Florence, Italy*

Abstract

Peak amplitude measurements of the fundamental mode of oscillation of a suspended aluminum alloy bar hit by an electron beam show that the amplitude is enhanced by a factor ~ 3.5 when the material is in the superconducting state. This result is consistent with the cosmic ray observations made by the resonant gravitational wave detector NAUTILUS, made of the same alloy, when operated in the superconducting state. A comparison of the experimental data with the predictions of the model describing the underlying physical process is also presented.

Key words: Gravitational wave detectors, Aluminum alloy, Superconductivity, Radiation acoustics

PACS: 04.80.Nn, 74.70.Ad, 61.82.Bg, 65.60.+a

¹ Present address: CSNSM, 91405 Orsay Campus, France

² Present address: Dept. of Physics, Univ. of Oxford, Oxford OX1 3PU, UK

1 Introduction

In a pioneering experiment [1] B.L. Baron and R. Hofstadter measured mechanical oscillations in piezoelectric disks when penetrating high energy electron beams impinged on the disks. The authors outlined the possibility that cosmic ray events could excite mechanical vibrations in a metallic cylinder at its resonant frequency and that they could represent a background for experiments aimed at the detection of gravitational waves (gw). The gw resonant detector NAUTILUS, a massive (2.3 t) suspended cylinder made of an aluminum alloy (Al5056) that can be cooled down to the thermodynamic temperature of 0.1 K, has been equipped with a cosmic ray detector to study the interactions due to cosmic rays and to provide a veto against the induced events in the antenna. The results on the cosmic ray observations made by NAUTILUS can be summarized as follows: 1) when the antenna was operated at a temperature $T = 0.14$ K, well below the transition temperature from normal-conducting (n) to superconducting (s) states of the material, the rate of high energy signals due to cosmic ray showers was larger than the expectations based on the model describing the underlying physical processes [2,3]; 2) there was no evidence of this feature when the antenna was operated at $T = 1.5$ K, well above the transition temperature [4]. From one side the hypothesis that this behavior was linked to the conducting state of the antenna and on the other side the incomplete knowledge at very low temperature of the thermophysical and thermodynamic parameters needed by the model have motivated an experiment (RAP) to measure the longitudinal oscillations of suspended cylindrical bars exposed to electron beam pulses of controlled energy and intensity. The experiment, performed at the Beam Test Facility (BTF) [5] of the DAFNE Φ -factory complex in the INFN Frascati Laboratory, has already obtained the following results: 1) the measurements over a wide temperature interval ($4.5 \text{ K} \leq T \leq 264 \text{ K}$) on a bar made of the same aluminum alloy as NAUTILUS have confirmed with good precision the validity of the model [6]; 2) the measurements on a pure niobium bar operated in the n and s state have demonstrated that the oscillation amplitude of the bar induced by the interaction with the beam depends on the state of conduction of the material [7].

In this letter we report on the measurements made on the aluminum alloy bar above and below the temperature of transition between the s and n state. In particular, we present a description of the model (Section 2), a summary of the experimental setup (Section 3), the collected data and analysis (Section 4) and the comparison between the data and the model (Section 5).

2 Discussion of the thermo-acoustic effects

A pressure pulse is generated in a suspended cylindrical bar in the n state following the interactions of an elementary particle with the bulk. This sonic pulse, due to the local thermal expansion caused by the warming up, related to the energy lost by the particle crossing the material, determines the excitation of the vibrational modes of the bar. In the experiment of Ref. [8] an aluminum bar was exposed to a proton beam and the theoretical expectations were based on a model in which the “amplitude of the fundamental longitudinal mode of oscillation”, hereafter referred to as Amplitude, is given by:

$$B_0 = \frac{2\alpha LW}{\pi c_V M} \quad (1)$$

for a beam hitting the center of the cylinder generatrix. In the previous relation L , M are respectively length, mass of the cylinder, W is the total energy loss of the beam in the bar, α is the linear thermal expansion coefficient and c_V is the isochoric specific heat. The ratio of the thermophysical quantities α and c_V is part of the definition of the Grüneisen parameter of the material:

$$\gamma = \frac{\beta K_T}{\rho c_V} , \quad (2)$$

where β is the volumetric thermal expansion coefficient ($\beta = 3\alpha$ for aluminum), K_T is the isothermal bulk modulus and ρ is the mass density. The parameter γ is a very slowly varying function of the temperature when the material is in the n state. Solution (1) is a particular case of a more general treatment of the problem, which includes the paths of the interacting particles in the bulk other than the coordinate of the impact point [9,10,11]. By the introduction of a vector field $\mathbf{u}(x,t)$ describing the local displacements from equilibrium, the amplitude of the mode k of the cylinder oscillation is proportional to:

$$\begin{aligned} g_k^{therm} &= \frac{\Delta P^{therm}}{\rho} \mathcal{A}' \mathcal{I}_k \\ &= \frac{\gamma}{\rho} \left| \frac{dW}{dx} \right| \mathcal{I}_k , \end{aligned} \quad (3)$$

where ΔP^{therm} is the pressure pulse due to the sonic source previously described, dW/dx is the specific energy loss of the interacting particle, \mathcal{A}' is the cross section of the tubular zone centered on the particle path in which the effects are generated and $\mathcal{I}_k = \int dl (\nabla \cdot \mathbf{u}_k(x))$ is a line integral over the particle path involving the normal mode of oscillation $\mathbf{u}_k(x)$. The Amplitude,

as given by (1), can be obtained starting from (3) for a thin bar ($R/L \ll 1$, where R is the bar radius) and for particles hitting the central section.

In the following, for the material in n state, we will compare the measured values of Amplitude to the expected value:

$$X_{therm} = B_0(1 + \epsilon) , \quad (4)$$

where ϵ is a corrective parameter estimated by a Monte Carlo (MC) simulation [6], which takes into account the solutions $O[(R/L)^2]$ for the modes of oscillation of a cylinder, the transverse dimension of the beam at the impact point and the trajectories of the secondary particles generated in the bar. The value of ϵ for the aluminum alloy bar used in the experiment is estimated by MC to be -0.04.

When the material is in the s state, an additional sonic source could be due to the local s - n transitions in zones centered around the interacting particle path [9,10]. The additional contribution to the amplitude of the cylinder oscillation mode k is proportional to:

$$\begin{aligned} g_k^{trans} &= \frac{\Delta P^{trans}}{\rho} \mathcal{A}'' \mathcal{I}_k \\ &= \frac{\gamma}{\rho} \left[K_T \frac{\Delta V}{V} + \gamma T \frac{\Delta \mathcal{S}}{V} \right] \mathcal{A}'' \mathcal{I}_k , \end{aligned}$$

where ΔV and $\Delta \mathcal{S}$ are the differences of the volume and entropy in the two states of conduction, while \mathcal{A}'' is the cross section of the tubular zone centered on the interacting particle path and switched from s to n state, which is given by $\mathcal{A}'' = (dW/dx)/(\Delta \mathcal{H}/V)$ [12,13] involving the difference of enthalpy, \mathcal{H} , among the two states. The differences can be expressed in terms of the thermodynamic critical field H_c and it follows, in first approximation, that [14,15]: $\Delta V/V = (V_n - V_s)/V = H_c(\partial H_c/\partial P)/(4\pi)$ and $\Delta \mathcal{S}/V = (\mathcal{S}_n - \mathcal{S}_s)/V = -H_c(\partial H_c/\partial T)/(4\pi)$. Moreover, by using the difference ($\Delta \mathcal{G}/V = (\mathcal{G}_n - \mathcal{G}_s)/V = H_c^2/(8\pi)$) of the Gibbs free energy among the two states and by making the hypothesis that H_c has the parabolic behavior $H_c(t) = H_c(0)(1 - t^2)$, where $t = T/T_c$ and T_c is the transition temperature, it follows that $\Delta \mathcal{H}/V = H_c^2(0)(1 - t^2)(1 + 3t^2)/(8\pi)$. In order to compare the observed data with the model predictions, we will use the ratio \mathcal{R} of the contributions to the Amplitude due to local transition effects (X_{trans}) and to thermal effects in the n state (X_{therm}). \mathcal{R} can be expressed as:

$$\mathcal{R} = \frac{X_{trans}}{X_{therm}} = \frac{g_0^{trans}}{g_0^{therm}}$$

$$= \left[\frac{K_T}{\gamma} \frac{\Delta V}{V} + T \frac{\Delta \mathcal{S}}{V} \right] \left[\frac{\Delta \mathcal{H}}{V} \right]^{-1}, \quad (5)$$

due to the existent proportionality between the mode amplitude and g .

In an alternative scenario, which takes into account that local transitions do not occur, the Amplitude expected values are given by the relation (4) making use of the α and c_V values for the s state.

3 Experimental setup

The experiment setup has been fully described in Ref. [6]. Here we briefly recall that the test mass is a cylindrical bar ($R = 0.091$ m, $L = 0.5$ m, $M = 34.1$ kg) made of Al5056, the same aluminum alloy (nominal composition 5.2 w% Mg and 0.1 w% of both Cr and Mn) used for NAUTILUS. The bar hangs from the cryostat top by means of a multi-stage suspension system insuring an attenuation on the external mechanical noise of -150 dB in the 1700-6500 Hz frequency window. The frequency of the fundamental longitudinal mode of oscillation of the bar is $f_0 = 5413.6$ Hz below $T = 4$ K. The cryostat is equipped with a ^3He refrigerator, capable of cooling the bar down to $T \sim 0.5$ K. The temperatures are measured inside the cryostat by 10 thermometers controlled by a multi-channel resistance bridge. In particular, a calibrated RuO_2 resistor detects the temperature of one of the bar end faces with an accuracy of 0.01 K for $T \lesssim 4$ K. Two piezoelectric ceramics (Pz), electrically connected in parallel, are inserted in a slot cut in the position opposite to the bar suspension point and are squeezed when the bar shrinks. In this Pz arrangement the strain measured at the bar center is proportional to the displacement of the bar end faces. The Pz output is first amplified and then sampled at 100 kHz by an ADC embedded in a VME system, hosting the data acquisition system. The measurement of the Pz conversion factor λ , relating voltage to oscillation amplitude, is accomplished according to a procedure based on the injection in the Pz of a sinusoidal waveform of known amplitude, with frequency f_0 and time duration less than the decay time of the mechanical excitations and on the subsequent measurement of Amplitude. The procedure is correct if $R/L \ll 1$ and a 6% systematic error in the determination of λ was found. Amplitude is measured according to $X = V_0^{\text{meas}}/(G\lambda)$, where G is the amplifier gain and V_0^{meas} is the maximum of the signal component at frequency f_0 , which is obtained by Fast Fourier Transform algorithms applied to the digitized Pz signals. The sign of Amplitude is taken positive or negative according to the sign of the first sampling above the noise in the waveform generated by the Pz and sampled by the ADC. BTF delivers to the bar single pulses of ~ 10 ns duration, containing N_e electrons of 510 ± 2 MeV energy. N_e ranges from about 5×10^7 to 10^9 and is measured with an accuracy of

$\sim 3\%$ (for $N_e > 5 \times 10^8$) by an integrating current transformer placed close to the beam exit point. MC, already introduced in Section 2, estimates an average energy lost $\langle \Delta E \rangle \pm \sigma_{\Delta E} = 195.2 \pm 70.6$ MeV for a 512 MeV electron interacting in the bar and, consequently, the total energy loss per beam pulse is given by $W = N_e \langle \Delta E \rangle$, $\sigma_W = \sqrt{N_e} \sigma_{\Delta E}$.

4 Measurements and data analysis

Samples of Al5056 obtained from the same production batch of the test mass have been used to characterize the material at very low temperatures. The measurement of the transition temperature to the s state conducted using the mutual inductance method gives the value $T_c = 0.845 \pm 0.002$ K and a total transition width of about 0.1 K. The smaller value of T_c with respect to pure Al (1.18 K) could be ascribed to the presence of Mn impurities in the alloy. In fact, experimental studies on AlMn polycrystalline alloys have shown that T_c was depressed down to 0.868 K and 0.652 K for Mn concentrations of 440 ppm and 900 ppm, respectively [16]. Moreover, Al50XX alloys contain inclusions of the extremely complex (MgAl) β phase [17] and the characterization of superconducting properties of the alloy $\beta - \text{Al}_3\text{Mg}_2$ shows that $T_c = 0.87$ K [18]. Specific heat data for Al5056 are available in literature [19], however, in order to completely characterize the production batch, we have performed c_V measurements above and below T_c (Fig. 1) using the calorimetric method of Ref. [20]. In the temperature interval $0.9 \text{ K} \leq T \leq 1.5 \text{ K}$ the fit of the data points, which have an accuracy of 5%, to the function $c_V/T = \Gamma + BT^2$ gives the values $\Gamma = 1157 \pm 31 \text{ erg cm}^{-3} \text{ K}^{-2}$ for the electronic specific heat coefficient per unit volume in the n state and $B = 0.14 \pm 0.01 \text{ mJ mol}^{-1} \text{ K}^{-4}$ for the lattice contribution. If the superconducting properties of Al5056 can be described by the BCS theory, then $H_c(0) \approx 2.42 \Gamma^{1/2} T_c \approx 70$ Oe. An independent check of the $c_V(T)$ behavior is obtained by the measurements at the bar end face of the temperature increments due to energy released by each beam pulse. The main features of the $c_V(T)$ behavior, as obtained by the calorimetry, are well reproduced by this method (inset of Fig. (1)).

The full set of Amplitude measurements (X) normalized to the energy deposited per beam pulse (W) in the explored temperature interval is shown in Fig. 2. For $T \geq 0.9$ K, above T_c , X has a strict linear dependence on W , as expected from the relation (1). The linear fit $X = bW$ (Fig. 3) gives $b = (2.42 \pm 0.17) 10^{-10} \text{ m/J}$, where the error is determined by the quadrature of the beam monitor (3%) and λ determination (6%) accuracies. The onset at $T \sim 0.9$ K and the behavior of the superconducting effects are shown in Fig. 2. As T decreases, the normalized Amplitude becomes negative, indicating that a compression rather than an expansion is generated by the beam interaction in the bulk. Its absolute values is greater than b , the normalized Amplitude

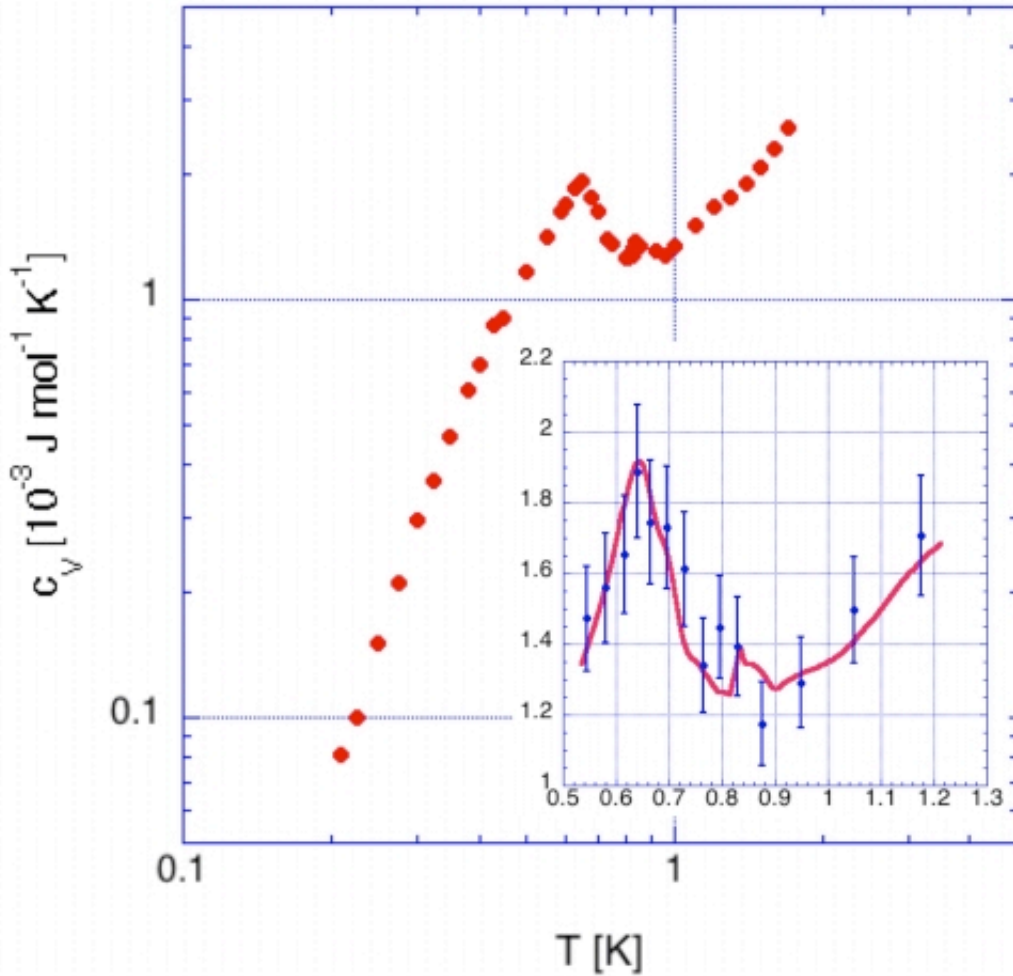


Fig. 1. *Al5056 specific heat: calorimetric measurements (5% accuracy). The inset shows the calorimetric measurements interpolated by a polynomial (continuous line) and the independent c_V determination based on the temperature increments at one end face of the bar (dots).*

value measured in the n state. The increase in the absolute value of the Amplitude explains the effects seen in cosmic ray observations by NAUTILUS, when operated at $T = 0.14$ K, as due to the conduction state of the material.

Furthermore, X does not linearly depend on W at fixed T , opposite to what has been observed [7] in pure Nb in the s state. The dependence of X/W on W in the s state is shown in Fig. (4) representing the data in four non-overlapping bands of W . This fact has an impact on the quantification of the enhancement of the absolute value of the Amplitude below and far away from T_c . Fig. 5 shows the averages of $|X/W|$ and W in four bins of data collected in the temperature interval ranging from 0.55 to 0.60 K, together with the best fit given by the exponential $\langle |X/W| \rangle = (8.31 \pm 2.88)10^{-10} e^{(-26.2 \pm 6.3)(W)}$ m/J. The average energy deposited by the cosmic rays interacting in the NAUTILUS

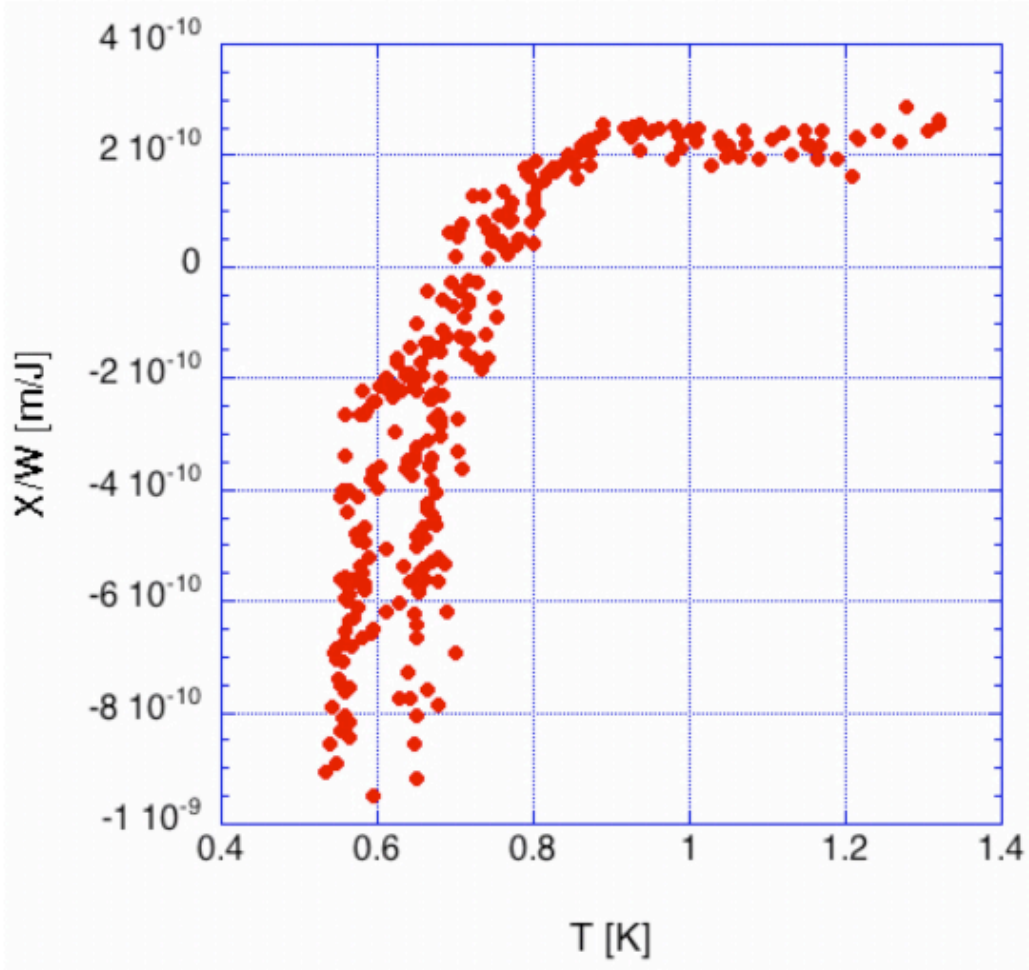


Fig. 2. Measured values of Amplitude (X) normalized to the energy (W) deposited in the bar per beam pulse vs. temperature (T).

antenna is in the order of 10^{-8} J [21], much lower than that released in our test mass by the beam pulse. We use the ratio $\mathcal{F} = \langle |X/W| \rangle / b$ as a factor quantifying the Amplitude enhancement in the s state with respect to the n one. With reference to Fig. (5), we obtain $\mathcal{F} = 3.4 \pm 1.2$ by the extrapolation of the fitting exponential to $\langle W \rangle = 10^{-8}$ J. A value of $\mathcal{F} \sim 3.5$ is consistent with the cosmic ray observations made by NAUTILUS in the s state [21].

5 Comparison with the model

The Amplitude (X) linearly depends on the deposited energy (W) in the model described in Section 2, while a X/W dependence on W is observed in the data. Therefore, we try to compare the model predictions to the data in the hypothesis that the linear dependence of X on W is attained at very low values of energy deposition. The application of the model for the expected value

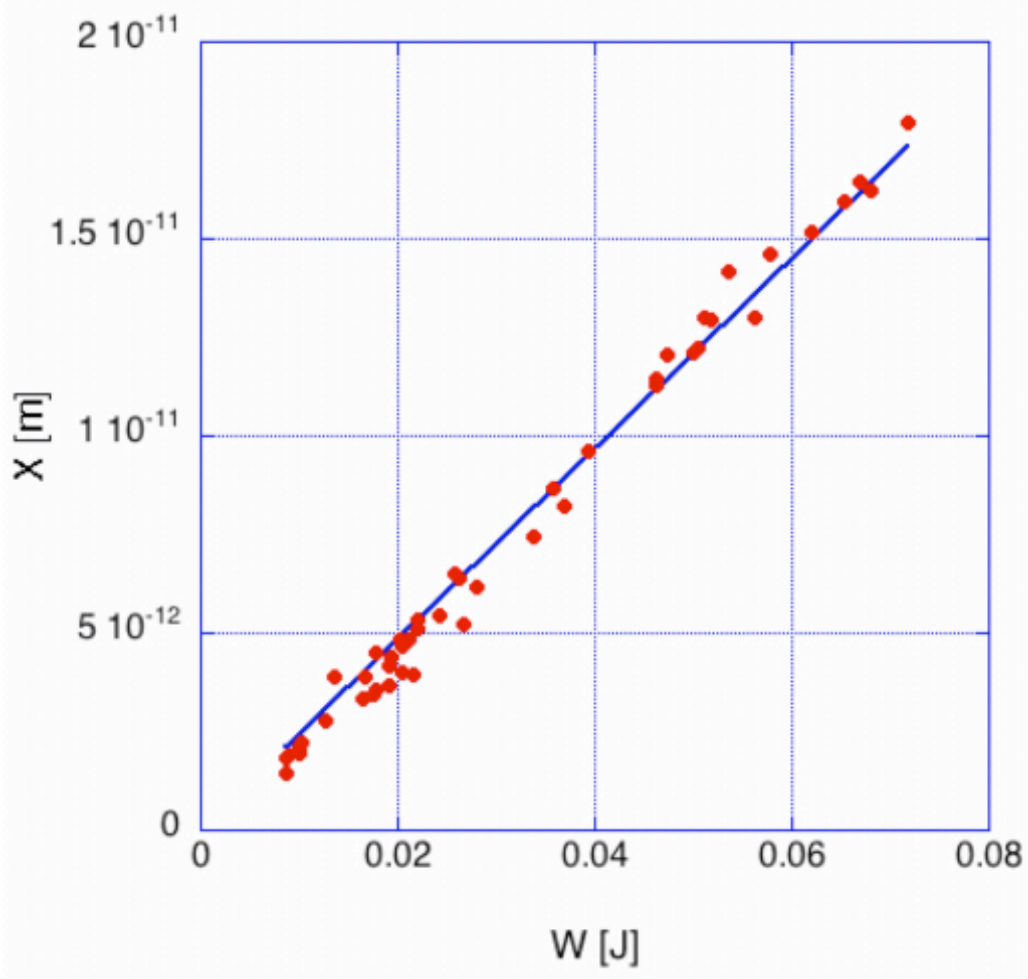


Fig. 3. $T \geq 0.9$ K (n state); Measured values of Amplitude (X) vs. the energy deposited per beam pulse (W). The slope of the fitted line is $b = 2.42 \cdot 10^{-10}$ m/J.

(X_{exp}) computation of the Amplitude in the s state requires the knowledge of 1) the thermophysical parameters α_n and $c_{V,n}$ of the material in order to evaluate X_{therm} for the n state below T_c and 2) the dependence of H_c on T and P for calculating X_{trans} via H_c and its derivatives $\partial H_c/\partial T$ and $\partial H_c/\partial P$. The use of relations (1), (2), (4) and (5) allow us to write:

$$\begin{aligned} \frac{X_{exp}}{W} &= \frac{X_{therm}}{W} (1 + \mathcal{R}) \\ &= \frac{X_{therm}}{W} \left\{ 1 + \left[\Lambda \frac{\Delta V}{V} + T \frac{\Delta S}{V} \right] \left[\frac{\Delta \mathcal{H}}{V} \right]^{-1} \right\} \end{aligned} \quad (6)$$

with:

$$\Lambda = \frac{2\rho L(1 + \epsilon)}{3\pi M \frac{X_{therm}}{W}}$$

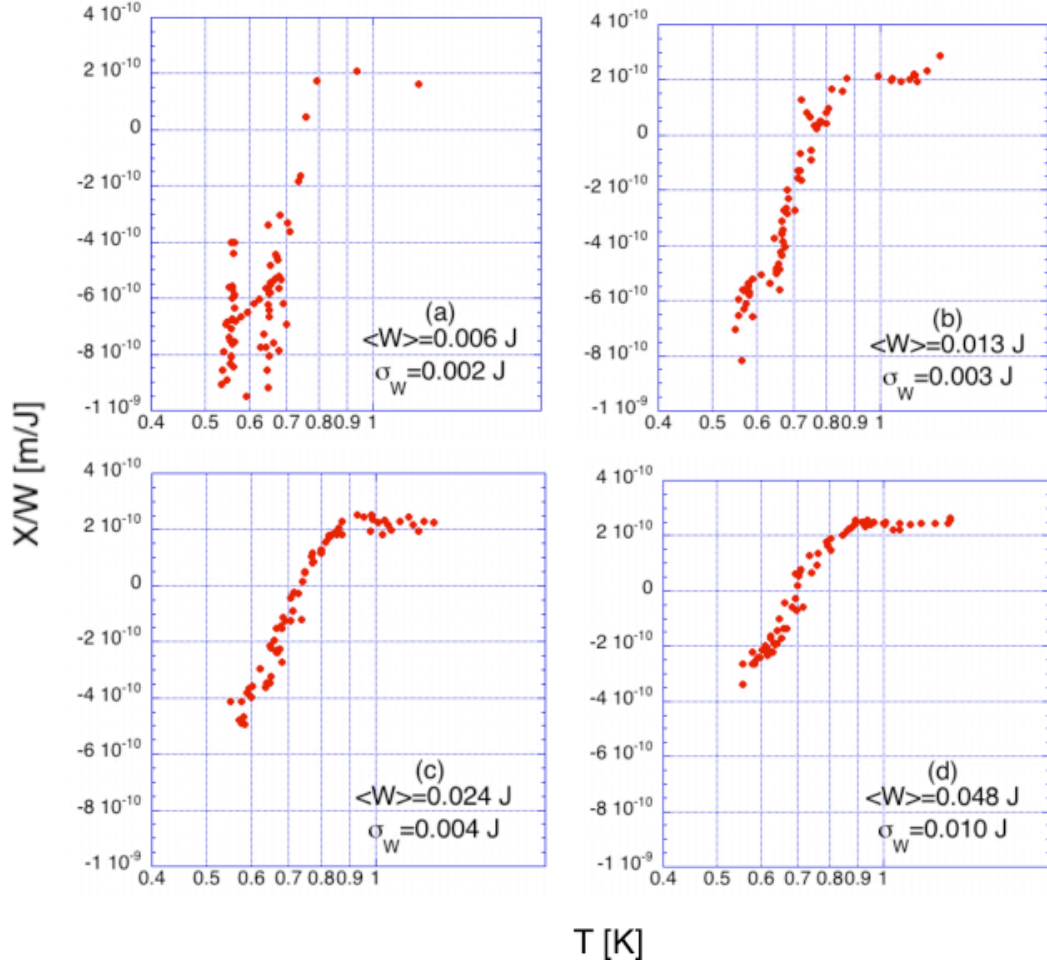


Fig. 4. Data of Fig. (2) ordered in 4 bands of deposited energy. Each band is identified by $\langle W \rangle \pm \sigma_W$. A dependence of X/W on W can be seen in the s state, e.g. at $T=0.6$ K.

The requirement 1) cannot be fulfilled due to the lack of knowledge of α_n for Al5056 and we therefore assume that $X_{therm}/W = b$ also in the temperature interval $0.5 \text{ K} \lesssim T \leq T_c$, due to the fact that γ_n , in this interval, is expected to have almost the same value as that assumed at slightly higher temperatures. In relation to requirement 2), we derive $\partial H_c/\partial T$ at $T < T_c$ from the H_c parabolic dependence on t , assuming that the unknown dependence of $\partial H_c/\partial P$ on t at $P = 0$ for Al5056 is equal to that of pure Al. Under this hypothesis, $\partial H_c/\partial P$ can be deduced by interpolating the tabulated values of H_c as a function of T and P contained in Ref. [22]. Inserting numerical values in relation (6) gives an average of $\langle X_{exp}/W \rangle = (-18 \pm 1)10^{-10} \text{ m/J}$ in the interval $0.55 \leq T \leq 0.6 \text{ K}$, where the error does not include systematic contributions deriving from the assumptions made. This is to be compared to $\langle X/W \rangle = (-8.3 \pm 2.8)10^{-10} \text{ m/J}$, obtained at $W = 10^{-8} \text{ J}$ from the measurements in the same temperature range (see Fig.(5)). This discrepancy can be ascribed to the fact that the model, as mentioned by the authors of Ref. [10], considers

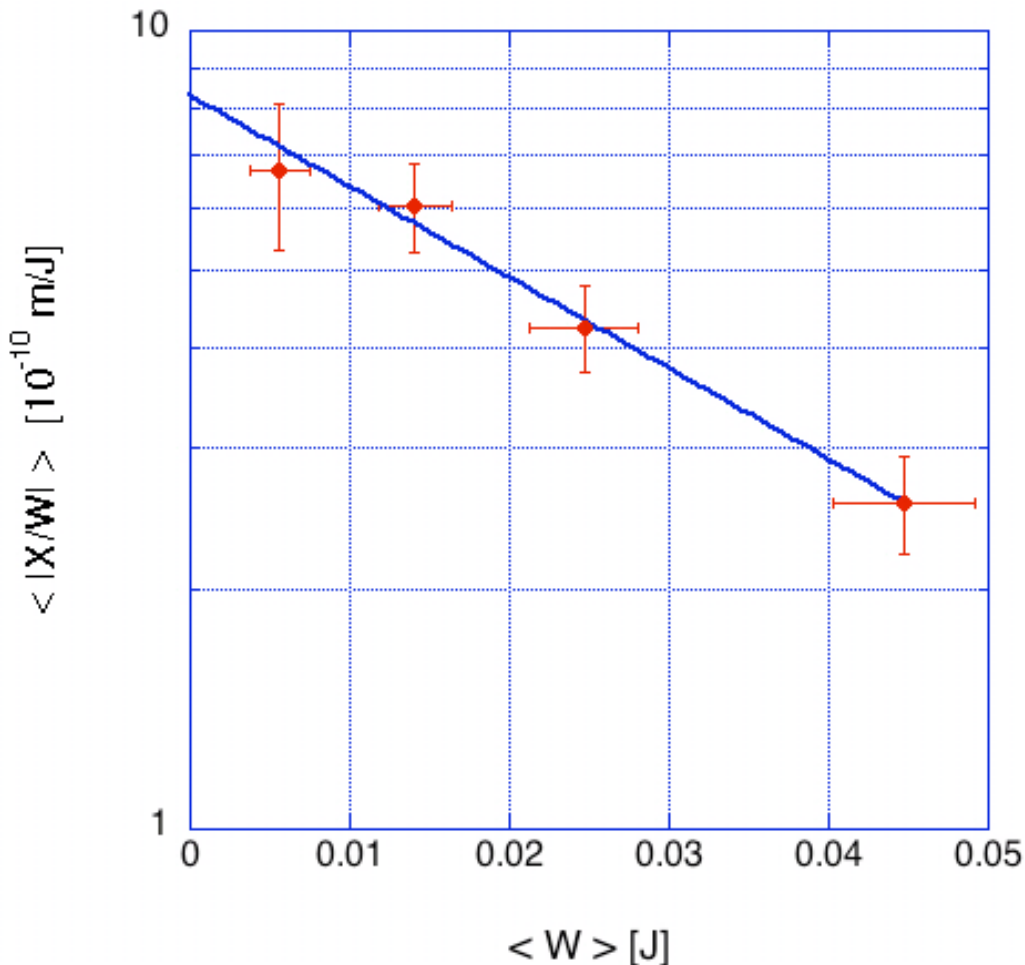


Fig. 5. $0.55 \leq T \leq 0.60 \text{ K}$; averages of the normalized absolute values of Amplitude $\langle |X/W| \rangle$ vs. the the average energy released per beam pulse $\langle W \rangle$. The line represents the fit given by $8.31 \cdot 10^{-10} e^{-26.2\langle W \rangle} \text{ m/J}$.

superconducting effects in pure materials, while the intrinsic properties of an alloy could determine additional contributions to the expected values of the oscillation amplitudes. Indeed, the model has given a satisfactory description of the behavior of the experimental data collected with a pure Nb test mass in the s state [7].

The calculation of X_{exp}/W for the s state, in the framework of the alternative scenario described in Section 2, requires the knowledge of $\alpha_s (= \alpha_s^e + \alpha^r$, where e and r refer to the electronic and lattice contributions, respectively) and $c_{V,s}$, the former being unknown and the latter measured. The relation (2) gives $\alpha_s^e = \rho c_{V,s}^e \gamma_s^e / (3K_T)$ and $\alpha^r = \rho c_V^r \gamma^r / (3K_T)$. Again, for lack of better knowledge, we presume the values of the Grüneisen parameters and of K_T for AL5056 to be similar to those of pure Al. Thus, we use $\gamma^r = 2.6$ [23] in the limit $t \rightarrow 0$, $\gamma_s^e = -11.5 \pm 1.0$ at $t \sim 0.7$ [24] and $K_T = 79.4 \cdot 10^9 \text{ N/m}^2$ near $T=0$ [25]. The insertion of these values in relation (4) gives $\langle X_{exp}/W \rangle = (-11 \pm 1) 10^{-10} \text{ m/J}$

in the same temperature interval as in the first scenario. As previously, the error is determined only by propagating the errors on the quantities in the right side of relation (4). The systematic uncertainties introduced in the calculations of the expected values in both scenarios do not allow us to individuate the one that better agrees with the experimental data. Moreover, it is interesting to derive the predictions at temperature values close to the lower limits of T in the $H_c(P, T)$ tabulation of Ref. [22]: $X_{exp}/W = (-28 \pm 1)10^{-10}$ m/J at $T = 0.3$ K in the first scenario and $X_{exp}/W = (-28 \pm 16)10^{-10}$ m/J in the alternative scenario, where for the latter the large error is due to the uncertainty on γ_s^e at this temperature.

Finally, dissipative effects, which can be inherent in this alloy and due to the flux line motion with consequent entropy transport, could play a role in the Amplitude observed values. A clue in this direction lies in the fact that Amplitude is not linearly dependent on W in the s state at fixed T .

6 Conclusions

The measurements performed on an Al5056 suspended bar, hit by an electron beam and operated at temperatures above and below T_c , have shown that in the s state, the amplitude of the fundamental mode of the bar is enhanced with respect to the n state by a factor ~ 3.5 at $T \sim 0.5$ K. This factor is consistent with the observations made by NAUTILUS on cosmic rays at $T = 0.14$ K. The amplitude change in the s state, following an energetic particle interaction, is due to the superconducting properties of the material. The absolute value of the normalized Amplitude is enhanced in the Al alloy and reduced in Nb. Incomplete knowledge of the involved thermophysical and thermodynamic parameters does not allow a full assessment of the model describing the underlying physical process in the s state. The effects due to cosmic ray interactions could be an important source of noise in future gw acoustic and interferometric detectors of improved sensitivities and a complete characterization of the thermo-acoustic effects in the test masses operated in the s state should be performed by direct measurements of the type shown in this letter.

Acknowledgements

We thank Messrs. F. Campolungo, M. Iannarelli and R. Lenci, which helped with the experiment setup.

This work is partially supported by the EU Project ILIAS (RII3-CT-2004-

506222).

References

- [1] B. L. Beron and R. Hofstadter, *Phys. Rev. Lett.* **23** (1969) 184
- [2] P. Astone, et al., *Phys. Rev. Lett.* **84** (2000) 14
- [3] P. Astone, et al., *Phys. Lett. B* **499** (2001) 16
- [4] P. Astone, et al., *Phys. Lett. B* **540** (2002) 179
- [5] G. Mazzitelli, et al., *Nucl. Instrum. Meth. A* **515**(2003) 524
- [6] B. Buonomo, et al., *Astropart. Phys.* **24** (2005) 65
- [7] M. Bassan et al., *Europhys. Lett.* **76** (2006) 1
- [8] A.M. Grassi Strini, G. Strini and G. Tagliaferri, *J. Appl. Phys.* **51** (1980) 948
- [9] A.M. Allega and N. Cabibbo, *Lett. Nuovo Cim.* **38** (1983) 263
- [10] C. Bernard, A. De Rujula and B. Lautrup, *Nucl. Phys. B* **242** (1984) 93
- [11] G. Liu and B. Barish, *Phys. Rev. Lett.* **61** (1988) 27
- [12] N.K. Sherman, *Phys. Rev. Lett.* **8** (1962) 438
- [13] B. Strehl, et al., *Phys. Lett. B* **242** (1990) 285
- [14] R.R Hake, *Phys. Rev.* **166** (1968) 471
- [15] We keep the practical cgs unit for the magnetic field, as used by the authors of the cited articles, and we convert the density of the magnetic energy to SI units.
- [16] F.W. Smith, *J. Low Temp. Phys.* **6** (1972) 435
- [17] R.L. Powell, W.J. Hall and H.M. Roder, *J. Appl. Phys.* **31** (1960) 496
- [18] E. Bauer, et al., *Phys. Rev. B* **76** (2007) 014528
- [19] E. Coccia and T.O. Niinikoski, *J. Phys. E: Sci. Instrum.* **16** (1983) 695
- [20] M. Barucci, et al., *Cryogenics* **46** (2006) 767
- [21] P. Astone, et al., *Astropart. Phys.* **30** (2008) 200
- [22] E.F. Harris and D.E. Mapother, *Phys. Rev.* **165** (1968) 522
- [23] T.H.K. Barron. J.C. Collins and G.K. White, *Adv. Phys.* **29** (1980) 609
- [24] A. Marini, *J. Low Temp. Phys.* **133** (2003) 313
- [25] G. N. Kamm and G. A. Alers, *J. Appl. Phys.* **35** (1964) 327